STRUCTURAL SCIENCE
CRYSTAL ENGINEERING
MATERIALS

ISSN: 2052-5206
journals.iucr.org/b

First experimental charge density study using a Bruker CMOS-type PHOTON 100 detector: the case of ammonium tetraoxalate dihydrate. Addendum

Katarzyna N. Jarzembska, Radosław Kamiński, Łukasz Dobrzycki and Michał K. Cyrański

Acta Cryst. (2015). B**71**, 241–243

Acta Cryst B
STRUCTURAL SCIENCE
CRYSTAL ENGINEERING
MATERIALS
ISSN 2052-5206

First experimental charge density study using a Bruker CMOS-type PHOTON 100 detector: the case of ammonium tetraoxalate dihydrate. Addendum

Katarzyna N. Jarzembska,[a,b]* Radosław Kamiński,[b] Łukasz Dobrzycki[a]* and Michał K. Cyrański[a]

[a]Czochralski Laboratory of Advanced Crystal Engineering, Biological and Chemical Research Centre, Department of Chemistry, University of Warsaw, Żwirki i Wigury 101, 02-089 Warsaw, Poland, and [b]Department of Chemistry, University at Buffalo, The State University of New York, Buffalo, NY 14260-3000, USA. *Correspondence e-mail: katarzyna.jarzembska@gmail.com, dobrzyc@chem.uw.edu.pl

Received 16 November 2014
Accepted 19 January 2015

Keywords: CMOS technology; PHOTON 100 detector; charge density distribution; quantum theory of atoms in molecules.

Addendum to Jarzembska *et al.* [*Acta Cryst.* (2014), B**70**, 847–855].

Very recently we published a paper describing the first use of a Bruker AXS CMOS-type PHOTON 100 detector in experimental electron density studies (Jarzembska *et al.*, 2014). A crystal of ammonium tetraoxalate dihydrate had been chosen as a test case due to its structural complexity, low symmetry and presence of anharmonic motion. Unfortunately, it transpires that we have overlooked a very important reference, namely the article published by Stash *et al.* (2013). The corresponding CIF was not present in the standalone version of the Cambridge Structural Database (Allen, 2002) available at the time we published our contribution. The paper by Stash *et al.* (2013) deals with the charge density distribution of the same compound, but measured at the 15-ID ChemMatCARS beamline of the Advanced Photon Source synchrotron (Chen *et al.*, 2014). Consequently, in this short addendum we would like to supplement our previous work by comparing the two charge density distributions. Such a comparison is especially valuable since the data had been measured using a well established methodology applying a Bruker AXS CCD-type APEX II detector at a synchrotron beamline known for accurate and precise electron density studies. Selected parameters of the two data collections are summarized in Table 1.

Stash *et al.* (2013) described the electron density of ammonium tetraoxalate dihydrate obtained at 15 K. This data collection temperature constitutes a significant difference compared to our study conducted at 100 K. Therefore, as expected, the following observations can be made:

(i) the unit cell is larger at 100 K than at 15 K;

(ii) at lower temperature anharmonic corrections for one of the O atoms (namely O10 in our original paper) are not necessary.

The latter shows that the effect observed on O10 at 100 K can be indeed attributed to the anharmonic thermal motion rather than disorder or other effects. The use of Gram–Charlier parameters (Johnson, 1969; Kuhs, 1983; Scheringer, 1985) in the charge density distribution refinement is therefore justified. It can also be noted that at higher temperature the extinction correction was not necessary, which may result from

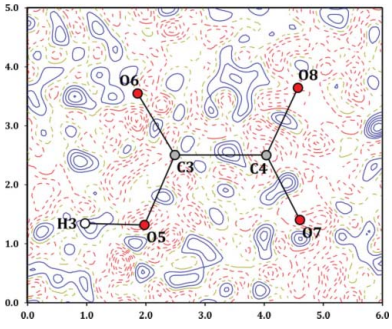

Table 1
Selected parameters characterizing the X-ray data collection in both cases.

	Article by Jarzembska *et al.* (2014)	Article by Stash *et al.* (2013)
Detector	PHOTON 100 (CMOS)	APEX II (CCD)
Radiation type	Mo sealed tube	Synchrotron
Wavelength, λ (Å)	0.71073	0.41328
Crystal size (mm)	0.24 × 0.21 × 0.09	0.03 × 0.06 × 0.07
T (K)	100	15
a (Å)	6.2372 (4)	6.1993 (3)
b (Å)	7.1935 (5)	7.1894 (3)
c (Å)	10.4745 (7)	10.4452 (4)
α (°)	94.5207 (18)	94.659 (1)
β (°)	99.8882 (18)	99.758 (1)
γ (°)	96.7177 (19)	96.653 (1)
V (Å^3)	457.45 (5)	453.31 (3)
$(\sin\theta/\lambda)_{max}$ (Å^{-1})	1.25	1.25
No. of measured reflections	50 285	58 907
No. of unique reflections	14 225	12 930
R_{mrg}†	0.0273	0.055
$R[F]$	0.0181‡	0.0232§
S	0.891‡	1.083§

† Definition of the R_{mrg} factor is summarized in the supporting information to our original article (Jarzembska *et al.*, 2014). ‡ Values given for all data (14 225 reflections). § Values given for 10 121 reflections with $I > \sigma(I)$.

Table 2
Fragment Bader charges ($\sum_i Q_i$) for molecular species present in the crystal lattice.

Fragment	$\sum_i Q_i$ (e)[a]	$\sum_i Q_i$ (e)[b]
$C_2H_2O_4$ (first)†	+0.01	−0.12
$C_2H_2O_4$ (second)‡	−0.02	−0.26
$C_2HO_4^-$	−0.93	−0.82
NH_4^+	+0.91	+0.89
H_2O (first)§	+0.04	−0.03
H_2O (second)¶	+0.00	+0.11

References: (*a*) Our paper (Jarzembska *et al.*, 2014); (*b*) Stash *et al.* (2013). † Oxalic acid molecule: 2 × (C1, O1, O2, H1). ‡ Oxalic acid molecule: 2 × (C2, O3, O4, H2). § Water molecule: O9, H8, H9. ¶ Water molecule: O10, H10, H11.

Table 3
Selected QTAIM parameters of covalent bonds at BCPs detected in both published crystal structures (d – bond distance, ϱ – electron density).

		Article by Jarzembska *et al.* (2014)			Article by Stash *et al.* (2013)†		
Fragment	Bond	d (Å)	$\varrho(\mathbf{r}_{BCP})$ (e Å^{-3})	$\nabla^2\varrho(\mathbf{r}_{BCP})$ (e Å^{-5})	d (Å)	$\varrho(\mathbf{r}_{BCP})$ (e Å^{-3})	$\nabla^2\varrho(\mathbf{r}_{BCP})$ (e Å^{-5})
$C_2H_2O_4$ (first)‡	C1—O1	1.2879 (3)	2.48	−27.4	1.286 (3)	2.51	−31.0
	C1—O2	1.2238 (3)	2.91	−27.1	1.221 (3)	2.79	−27.4
	C1—C1^{i}	1.5398 (2)	1.73	−13.4	1.537 (4)	1.72	−13.3
$C_2H_2O_4$ (second)§	C2—O3	1.2860 (3)	2.47	−27.9	1.283 (3)	2.43	−27.0
	C2—O4	1.2266 (3)	2.91	−30.6	1.225 (3)	2.90	−33.2
	C2—C2^{ii}	1.5490 (1)	1.72	−13.4	1.546 (4)	1.76	−13.9
$C_2HO_4^-$	C3—O5	1.2970 (3)	2.44	−26.7	1.294 (3)	2.55	−34.6
	C4—O7	1.2428 (3)	2.74	−25.9	1.243 (3)	2.51	−31.0
	C4—O8	1.2608 (3)	2.67	−29.2	1.258 (3)	2.79	−27.4
	C3—C4	1.5507 (2)	1.68	−12.0	1.550 (3)	1.75	−13.7

Symmetry codes: (i) $-x+2, -y+2, -z+1$; (ii) $-x, -y+1, -z+1$. † All values are rounded for easier comparison. ‡ Oxalic acid molecule: 2 × (C1, O1, O2, H1). § Oxalic acid molecule: 2 × (C2, O3, O4, H2).

the increased mosaicity of a crystal. However, higher mosaicity may also be attributed to some extent to the size of a crystal and a higher number of imperfections, due to different synthesis procedures.

It is valuable to compare the modelled electron density distributions on the basis of the Bader quantum theory of atoms in molecules (QTAIM) analysis performed in both cases. The integrated fragment charges of all molecular species are summarized in Table 2. General conclusions are basically the same in both cases, that is:

(i) water molecules are almost neutral;

(ii) oxalic acid molecules are either slightly negative or can be considered neutral;

(iii) formal +1 and −1 charges are well localized on the NH_4^+ cation and oxalate anion, respectively.

We attribute the differences between charges in both data sets to different data collection and refinement schemes, different temperatures and a different accuracy of integration.

More information is needed though to comment on the respective atomic charges obtained from both charge density analyses. Despite the similarity of the fragment charges, atomic charges between the two measurements differ quite considerably. For example, whereas the NH_4^+ Bader charges are very consistent (Table 3), the charges on the N atoms are equal to −1.73 and −1.26 e in our paper and that by Stash *et al.* (2013), respectively. This can be explained by the fact that the total electron density distribution was modelled using the least-squares procedure (thus atomic charges are dominated by the refined values of P_v parameters), which may lead to discrepancies between the individual values but, at the same time, provides a comparable general picture. Similar behaviour was observed by Martin & Pinkerton (1998) in their early comparison of CCD and point-detector data sets.

It is also worth comparing bond lengths and typical properties evaluated at bond critical points (BCP). These are presented briefly in Table 3. The slight discrepancies between the bond lengths obtained result most probably from different measurement temperatures. On the other hand, BCP properties match quite well. We note, however, that in the case of the CMOS data we observed some minor differences between the oxalic acid molecules and oxalate anions in terms of properties of the C—C and C—O bonds, which are less pronounced for the synchrotron data. Nevertheless, considering the realistic method precision, estimated in one of our previous articles (Kamiński *et al.*, 2014), the differences are negligible which makes the two charge density distributions consistent.

Additionally, the high similarity of both static electron density distributions supports a proper thermal motion deconvolution *via* the application of the Hansen–Coppens model (Hansen & Coppens, 1978). Furthermore, using the CMOS detector data we were able to reproduce the polarization of the O-bound hydrogen atoms, as well as similar Laplacian

distributions around the NH_4^+ cation, which is well visible when comparing the respective Laplacian maps.

Finally, we recall that our original contribution was focused on testing the feasibility of a new PHOTON 100 detector in experimental charge density studies. The current brief comparison with the excellent charge density results published by Stash *et al.* (2013) confirms that, despite some deficiencies in our data collection (*e.g.* rather high residual values after the refinement, overestimated weak reflection intensities), the data quality is high. This comparison is especially valuable considering those who were not convinced that CMOS-detector data can be successfully used for fine crystallographic studies. However, as pointed out in our original paper, more tests and comparisons are naturally needed to fully establish a proper methodology for accurate charge density studies when using a CMOS detector.

Acknowledgements

The X-ray measurement was performed in the Czochralski Laboratory of Advanced Crystal Engineering (Department of Chemistry, University of Warsaw) established by generous support from the Polish Ministry of Science and Higher Education (grant No. 614/FNiTP/115/2011). The research was founded by the National Science Centre (grant No. NCN 2011/03/B/ST4/02591). KNJ thanks the Polish Ministry of Science and Higher Education for financial support within the 'Mobility *Plus*' programme. Authors are indebted to Vladimir Tsirelson (Moscow, Russia) for pointing out the omission of his very important contribution.

References

Allen, F. H. (2002). *Acta Cryst.* B**58**, 380–388.
Chen, Y.-S., Brewer, H., Meron, M. & Viccaro, J. (2014). *Acta Cryst.* A**70**, C1727.
Hansen, N. K. & Coppens, P. (1978). *Acta Cryst.* A**34**, 909–921.
Jarzembska, K. N., Kamiński, R., Dobrzycki, Ł. & Cyrański, M. K. (2014). *Acta Cryst.* B**70**, 847–855.
Johnson, C. K. (1969). *Acta Cryst.* A**25**, 187–194.
Kamiński, R., Domagała, S., Jarzembska, K. N., Hoser, A. A., Sanjuan-Szklarz, W. F., Gutmann, M. J., Makal, A., Malińska, M., Bąk, J. M. & Woźniak, K. (2014). *Acta Cryst.* A**70**, 72–91.
Kuhs, W. F. (1983). *Acta Cryst.* A**39**, 148–158.
Martin, A. & Pinkerton, A. A. (1998). *Acta Cryst.* B**54**, 471–477.
Scheringer, C. (1985). *Acta Cryst.* A**41**, 79–81.
Stash, A. I., Chen, Y.-S., Kovalchukova, O. V. & Tsirelson, V. G. (2013). *Russ. Chem. Bull.* **62**, 1752–1763.